Cellular/Molecular

The Role of 5-HT$_3$ Receptors in Signaling from Taste Buds to Nerves

Eric D. Larson,[2,3]* Aurelie Vandenbeuch,[2,3]* Anja Voigt,[4] Wolfgang Meyerhof,[4] Sue C. Kinnamon,[2,3] and Thomas E. Finger[1,3]

[1]Department of Cell and Developmental Biology, [2]Department of Otolaryngology, and [3]Rocky Mountain Taste and Smell Center, University of Colorado School of Medicine, Aurora, Colorado 80045, and [4]Department of Molecular Genetics, German Institute of Human Nutrition Potsdam-Rehbruecke, 14588 Nuthetal, Germany

Activation of taste buds triggers the release of several neurotransmitters, including ATP and serotonin (5-hydroxytryptamine; 5-HT). Type III taste cells release 5-HT directly in response to acidic (sour) stimuli and indirectly in response to bitter and sweet tasting stimuli. Although ATP is necessary for activation of nerve fibers for all taste stimuli, the role of 5-HT is unclear. We investigated whether gustatory afferents express functional 5-HT$_3$ receptors and, if so, whether these receptors play a role in transmission of taste information from taste buds to nerves. In mice expressing GFP under the control of the 5-HT$_{3A}$ promoter, a subset of cells in the geniculate ganglion and nerve fibers in taste buds are GFP-positive. RT-PCR and *in situ* hybridization confirmed the presence of 5-HT$_{3A}$ mRNA in the geniculate ganglion. Functional studies show that only those geniculate ganglion cells expressing 5-HT$_{3A}$-driven GFP respond to 10 μM 5-HT and this response is blocked by 1 μM ondansetron, a 5-HT$_3$ antagonist, and mimicked by application of 10 μM m-chlorophenylbiguanide, a 5-HT$_3$ agonist. Pharmacological blockade of 5-HT$_3$ receptors *in vivo* or genetic deletion of the 5-HT$_3$ receptors reduces taste nerve responses to acids and other taste stimuli compared with controls, but only when urethane was used as the anesthetic. We find that anesthetic levels of pentobarbital reduce taste nerve responses apparently by blocking the 5-HT$_3$ receptors. Our results suggest that 5-HT released from type III cells activates gustatory nerve fibers via 5-HT$_3$ receptors, accounting for a significant proportion of the neural taste response.

Key words: 5ht3; barbiturate; calcium; geniculate ganglion; serotonin; taste signaling

Significance Statement

Historically, serotonin (5-hydroxytryptamine; 5-HT) has been described as a candidate neurotransmitter in the gustatory system and recent studies show that type III taste receptor cells release 5-HT in response to various taste stimuli. In the present study, we demonstrate that a subset of gustatory sensory neurons express functional 5-HT$_3$ receptors that play a significant role in the neurotransmission of taste information from taste buds to nerves. In addition, we show that the anesthetic pentobarbital, widely used in taste nerve recordings, blocks 5-HT$_3$ signaling. Therefore, many conclusions drawn from those data need to be reexamined in light of this anesthetic effect.

Introduction

Taste buds contain several types of chemosensory cells and are innervated by multiple nerve fibers. All taste fibers express ionotropic purinergic (P2X) receptors (Bo et al., 1999; Ishida et al., 2009) that are required for transmission from taste receptor cells to the afferent nerves; genetic deletion or pharmacological blockade of the P2X$_2$ and P2X$_3$ receptors expressed by the gustatory nerve fibers eliminates chorda tympani nerve responses to all taste stimuli (Finger et al., 2005; Ohkuri et al., 2012; Jaber et al., 2014; Vandenbeuch et al., 2015). Sweet, umami, and bitter tastants stimulate type II receptor cells to release ATP (Huang et al., 2005, 2009), thereby activating sensory afferents. Sour tastants (acids) and high concentrations of NaCl stimulate type III taste cells (Huang et al., 2006, 2008), yet no one has succeeded in

Received May 14, 2015; revised Oct. 13, 2015; accepted Nov. 5, 2015.

Author contributions: E.D.L., A. Vandenbeuch, A. Voigt, W.M., S.C.K., and T.E.F. designed research; E.D.L., A. Vandenbeuch, A. Voigt, and T.E.F. performed research; E.D.L., A. Vandenbeuch, A. Voigt, W.M., S.C.K., and T.E.F. analyzed data; E.D.L., A. Vandenbeuch, A. Voigt, W.M., S.C.K., and T.E.F. wrote the paper.

This work was supported by the National Institutes of Health [Grant R01DC012931 to T.E.F., Grant R01DC012555 to S.C.K., and Grant P30DC004657 to Dr. Diego Restrepo (University of Colorado, School of Medicine)], the Federal Ministry for Education and Research, and the Ministry for Science, Research and Culture of the State of Brandenburg, Germany (W.M.). We thank Nicole Schultz and Jason Parnes for help with tissue preparation for immunohistochemistry, Kyndal Davis for genotyping and maintaining the mouse colony, Catherine Anderson for assistance with RT-PCR experiments, Jennifer Stratford for assistance with statistical analysis, and Integral Molecular for the kind gift of anti-P2X$_3$ LM-021.

The authors declare no competing financial interests.

*E.D.L. and A.Vandenbeuch contributed equally to this work.

Correspondence should be addressed to Dr. Eric D. Larson, Department of Otolaryngology, University of Colorado Medical School, P15-7460D, MS 8606, 12700 E. 19th Ave, Aurora, CO 80045. E-mail: eric.larson@ucdenver.edu.

DOI:10.1523/JNEUROSCI.1868-15.2015

 0270-6474/15/3515984-12$15.00/0

Table 1. List of primers used for riboprobe generation (*in situ* hybridization, ISH) and in RT-PCR experiments

Gene	Primer sequence	Size	Accession no.
β-actin (PCR)	F: 5′-CACCCTGTGCTGCTCACC-3′ R: 5′-GCACGATTTCCCTCTCAG-3′	328 bp	NM_007393
5-HT_{3A} (PCR)	F: 5′-AACAGCTATGCAGAAATGAAGTT-3′ R: 5′-GGCTGACTGCGTAGAATAAAGG-3′	66 bp	NM_013561
5-HT_{3A} (for ISH)	F: 5′-GCCTTGACATCTACAACTTCCC-3′ R: 5′-GAGCAGTCATCAGTCTTGTTGG-3′	660 bp	NM_013561

measuring ATP release from these cells. Rather, sour tastants evoke release of serotonin (5-hydroxytryptamine; 5-HT) directly from type III cells (Huang et al., 2005, 2009). However, indirect release of 5-HT has been reported with sweet- and bitter-tasting stimuli (Meredith et al., 2015). Herein, we test whether 5-HT released by taste cells plays a role in the transmission of taste information by activation of 5-HT_3 receptors on afferent nerve fibers.

Only two 5-HT receptors have been identified in taste tissue: 5-HT_1 and 5-HT_3 (Herness and Chen, 2000; Kaya et al., 2004). 5-HT_1 receptors are expressed by type II taste cells and 5-HT_3 receptors are hypothesized to be expressed in gustatory nerve fibers (Jackson and Yakel, 1995; Wang et al., 2002). Whereas 5-HT_1 receptors are inhibitory G-protein-coupled receptors (Hoyer and Schoeffter, 1991), 5-HT_3 receptors are excitatory-ligand-gated ion channels that form pentameric combinations of the 5-HT_3 isoforms (5-HT_{3A}–5-HT_{3E}). Every functional 5-HT_3 receptor must contain at least one 5-HT_{3A} subunit (Jackson and Yakel, 1995; Hassaine et al., 2014).

5-HT released by type III taste cells activates adjacent type II taste cells that express the 5-HT_{1A} receptor, resulting in inhibition of type II cells (Herness and Chen, 2000; Huang et al., 2005; Jaber et al., 2014). The 5-HT released by type III cells could also activate 5-HT_3 receptors on afferent nerve fibers. Type III cells (but not type II cells) form traditional synapses with afferent nerve fibers (Kinnamon et al., 1985; Yee et al., 2001; DeFazio et al., 2006) and synthesize and store 5-HT (Dvoryanchikov et al., 2007) in dense-core synaptic vesicles located at these synaptic sites (Fujimoto et al., 1987). Therefore, 5-HT signaling to afferent nerve fibers could participate in the transmission of sour or some components of salty taste by type III cells.

In the present study, we examine the role of 5-HT_3 signaling in transmission of taste information. We used anatomical and molecular approaches to demonstrate expression of the 5-HT_{3A} subunit in taste ganglia and taste buds and then used physiological and pharmacological approaches to determine whether these receptors are functional and crucial in the taste system.

Materials and Methods

Animals. Mice were housed at the University of Colorado Anschutz Medical Campus or at the German Institute of Human Nutrition in ventilated cages on a 12 h/12 h light/dark cycle and fed standard chow *ad libitum*. All experimental procedures were approved by the Animal Care and Use Committee at the University of Colorado School of Medicine or the German Institute of Human Nutrition. Calcium imaging and anatomical experiments were conducted on tissue from 2- to 6-month-old male and female 5-HT_{3A}GFP mice originally on FVB/N-Swiss Webster background (STOCK Tg(Htr3a-EGFP)DH30Gsat/Mmnc; RRID:IMSR_MMRRC:000273) but crossed for 2–4 generations with the C57BL/6 line. Nerve recordings were conducted on 2- to 6-month-old male and female 5-HT_{3A}KO (Zeitz et al., 2002) mice bred on a C57BL/6J background (B6.129X1-Htr3a^{tm1Jul}/J; RRID:IMSR_JAX:005251; Jackson Laboratories) and male C57BL/6J WT (RRID:IMSR_JAX:000664) controls. RT-PCR and *in situ* hybridization experiments were conducted on tissue from 2- to 6-month-old male C57BL/6J mice. No differences due to sex were observed in any experiments. Genotyping of 5-HT_{3A}GFP and 5-HT_{3A}KO mice were done per distributor recommendations (MMRRC and Jackson Laboratory, respectively).

RT-PCR. RNA was extracted from geniculate ganglia of 5-HT_{3A}KO and WT mice (3 mice each) according to manufacturer's instructions using the RNeasy Micro kit (Qiagen), including a 30 min DNase I treatment at room temperature for removal of genomic DNA. Reverse transcription of 250 ng of RNA was performed using the iScript cDNA Synthesis kit (Bio-Rad). For every experiment, parallel reactions were set up in which the reverse transcriptase enzyme was omitted as a control to detect for DNA contamination. Ten percent (2 μl) of the RT-PCR product was added to the PCR (Qiagen TaqPCR Core kit).

Primer sequences for each PCR are described in Table 1. PCR primers for 5-HT_{3A} were designed in accordance with information from Jackson Laboratories and anneal in exon 7 and 8 (mutation location of 5-HT_{3A}KO; Table 1). PCR conditions for detection of both 5-HT_{3A} and β-actin included an initial 5 min denaturation step, followed by 35 cycles of 30 s denaturation at 95°C, 30 s annealing at 63°C, and 45 s extension at 72°C; concluding with a 7 min final extension step. We included cDNA from mouse whole brain (Clontech) and a no template control (water). Amplified sequences were visualized by gel electrophoresis in 2% agarose gels stained with GelRed (Biotium).

In situ *hybridization.* Using cDNA from brain and oligonucleotides shown in Table 1, we performed PCRs to generate probes for *in situ* hybridization. PCR conditions included an initial 10 min denaturation step, followed by 39 cycles of 1 min denaturation at 95°C, 30 s annealing at 64°C, and 1 min extension at 68°C, concluding with a 10 min final extension step. PCR products were sequenced and cloned into the transcription vector pBluescriptKS (Stratagene). Before *in vitro* transcription, we linearized the plasmids with appropriate restriction endonucleases and generated sense and antisense riboprobes using *in vitro* transcriptions (Roche Applied Science) with T7 polymerase and the DIG RNA labeling kit (Roche Diagnostics).

Frozen sections (14 μm) of mouse ganglia were cut (Microm), thaw mounted onto positively charged glass slides (Menzel), and stored at −80°C. Before hybridization, the sections were fixed with 4% paraformaldehyde in PBS (0.1 M phosphate buffer, pH 7.2, 0.9% saline) and then permeabilized with 0.2 M hydrochloric acid for 10 min and 1% Triton X-100 in PBS for 2 min. After acetylation by treatment with 0.1 M triethanolamine 0.25% acetic anhydride, pH 8.0, the tissue was prehybridized (prehybridization solution: 0.75 M NaCl, 25 mM PIPES, 25 mM EDTA, 5× Denhardt's reagent, 0.2% SDS, 250 μg/ml *Escherichia coli* tRNA, and 500 μg/ml salmon testis DNA, pH 6.8) at room temperature for 5 h. Riboprobes were incubated for 10 min at 85°C before application onto the sections and used for hybridization at a final concentration of 500 ng/ml. Hybridization was performed overnight at 56°C in a chamber humidified with 50% formamide. After hybridization, the slides were washed several times, followed by 30 min RNAase treatment (1 μg/ml RNase A in 0.5 M NaCl, 10 mM Tris-HCl, and 1.0 mM EDTA, pH 7.5) and additional washes with 1× SSC buffer at 45°C. To detect hybridized riboprobes, sections were incubated with an alkaline-phosphatase-conjugated anti-digoxigenin antibody (1:750; Roche Applied Science) for 1 h at room temperature. Colorimetric detection was accomplished with color substrate (0.175 mg/ml 5-bromo-4-chlor-indolyl-phosphate and 0.25 mg/ml nitroblue-tetrazolium-chloride) applied to the sections and incubated overnight at room temperature in darkness. On the following day, color reaction was stopped by a 5 min incubation in Tris-EDTA buffer. Sections were mounted with glass coverslips and images were taken using

Table 2. List of primary antisera

Target protein	Host	Dilution	Manufacturer	Catalog no.	RRID	Lot
GFP	Chicken	1:2000	Aves	GFP-1010	AB_2307313	0511FP12
GNAT3	Goat	1:500	Aviva System Biology	OAEB00418	AB_10882823	G2 E060911
Gustducin	Rabbit	1:5000	Santa Cruz	SC-395	AB_673678	H3112
$P2X_3$	Guinea pig	1:750	Neuromics	GP10108	AB_2283325	400911
$P2X_3$	Human	5 μg/ml	Integral Molecular	n/a	n/a	LM-021
Serotonin	Rabbit	1:5000	Immunostar	20080	AB_572263	924005

Both $P2X_3$ antisera were validated by lack of staining of tissue from $P2X_3$-KO mice. LM-021 is a humanized monoclonal antibody directed against the full-length protein using lipoparticle-based immunization (Banik et al., 2011).

Table 3. List of commercially available fluorescent secondary antisera used in this study

Target species	Host	Dilution	Manufacturer	Catalog no.	RRID	Wavelength
Chicken	Donkey	1:800	Jackson ImmunoResearch	703-475-155	AB_2340373	488
Chicken	Goat	1:800	Invitrogen	A11039	AB_142924	488
Goat	Donkey	1:800	Invitrogen	A21447	AB_141844	647
Guinea Pig	Donkey	1:800	Jackson ImmunoResearch	706-605-148	AB_2340476	647
Guinea Pig	Goat	1:800	Invitrogen	A11075	AB_141954	568
Human	Donkey	1:800	Jackson ImmunoResearch	709-295-149	AB_2340547	Rho-Red-X
Rabbit	Donkey	1:800	Invitrogen	A10042	AB_11180183	568
Rabbit	Goat	1:800	Invitrogen	A21245	AB_141775	647

a microscope (Axioplan; Zeiss) connected to a CCD camera (RT slider; Diagnostic Instruments).

Geniculate ganglion retrograde label. The geniculate ganglion houses the cell bodies of nerve fibers innervating taste buds of the anterior tongue and soft palate, as well as general cutaneous fibers innervating part of the external ear. The majority of cells of the geniculate ganglion are gustatory, contributing to the chorda tympani and greater superficial petrosal nerves (Foley and DuBois, 1943; van Buskirk, 1945) innervating, respectively, fungiform papillae and palatal taste fields. Somatosensory innervation of these taste fields arises from the trigeminal nerve; therefore, cells of the geniculate ganglion that innervate taste fields are gustatory rather than somatosensory in function.

To identify ganglion cells innervating palatal or fungiform taste buds, the retrograde tracer FluoroGold (Fluorochrome) was injected into the anterior tongue and soft palate using a protocol modified from King and Bradley (2000). Mice were anesthetized with intramuscular injections of dexmedetomidine hydrochloride (0.4 mg/kg; Pfizer), followed by ketamine hydrochloride (40 mg/kg; Bioniche Pharma). After a surgical level of anesthesia was obtained, the mouth was gently opened and 10–20 μl of a 5% FluoroGold solution in water was injected under taste epithelium using a Hamilton microsyringe (#701; Hamilton). Injection sites included the most anterior end of the tongue (fungiform papillae region), the lateral tongue (foliate papillae region), and the soft palate. Anesthesia was reversed with atipamezole (2 mg/kg; Pfizer) and mice were treated with 0.5% Marcaine (Hospira) during their postsurgical recovery. Five days after injection, the mice were reanesthetized with pentobarbital (FatalPlus 0.02 ml, i.p; Vortech) and then perfused transcardially with 4% paraformaldehyde in phosphate buffer (in mM/L: 29 NaH_2PO_4, 75 Na_2HPO_4, pH 7.2–7.4).

Immunohistochemistry. Tissues were harvested immediately after perfusion fixation with buffered 4% paraformaldehyde and postfixed in the same fixative for 2–4 h. All tissue was cryoprotected overnight with 20% sucrose in phosphate buffer and then cryostat sectioned at 12–16 μm. Some animals were injected intraperitoneally with 5-hydroxy-L-tryptophan (50 mg/kg; Sigma-Aldrich) 1 h before killing to increase 5-HT levels. The cryostat sections were immunoreacted overnight at 4°C with primary antibodies to label specific cell types and nerve fibers: GFP to label $5\text{-}HT_{3A}$GFP containing nerve fibers, GNAT3 (gustducin) to label a subpopulation of type II taste cells, $P2X_3$ to label nerve fibers, and 5-HT to label serotonin-accumulating type III taste cells. See Table 2 for details of antisera. The humanized monoclonal $P2X_3$ antibody was prepared using a lipoparticle approach (Banik et al., 2011) incorporating full-length human $P2X_3$ protein. Preparations lacking primary antisera were routinely run in parallel to test for specificity of secondary antisera. Specificity of the gustducin antiserum was tested on gustducin-knock-out mice and showed no staining. Similarly, the $P2X_3$ antibody was tested on tissue from $P2X_3$-knock-out mice and no signal was observed. Fluorescent secondary antibodies (Table 3) were reacted with tissue sections for 2 h at room temperature before mounting with Fluoromount G (Southern Biotech).

Z-stack images of taste buds and geniculate ganglia were collected on an Olympus Fluoview FV300 laser scanning confocal microscope with a 60× oil-immersion objective [numerical aperture (NA) 1.3] and 20× oil-immersion objective (NA 0.7) or on a Leica TCS SP5 laser scanning confocal microscope with a 63× oil-immersion objective (NA 1.4).

Quantification of geniculate ganglion cell labeling. Regions of interest in the perikaryon of individual ganglion cells (as identified by $P2X_3$ immunoreactivity) were outlined using ImageJ (RRID: nif-0000-30467). Average fluorescence intensity for each region of interest was measured in all channels. Background fluorescence, measured in a region absent of tissue, was subtracted from the measured value of each cell and these background-subtracted values were normalized to the maximum value of its respective channel. For quantification of FluoroGold labeling, cells were scored in a binary fashion (yes or no) for presence of FluoroGold and/or GFP. After fluorescence intensity normalization (where 0 is no expression and 1 is maximum), individual cells were scored in each channel (FluoroGold and GFP) as above or below a predetermined threshold. Threshold was determined by fitting bimodal distributions of intensity values with two peak Gaussian functions. The threshold for expression was defined as any value >2 SDs above the mean of the lower, background peak. Cells above threshold were considered positive for label. For quantitative analysis, only raw images were used. Images for manuscript display were adjusted with Photoshop (Adobe Systems) using only levels, brightness, and contrast modifications to the entire image.

Geniculate ganglion cell isolation. Geniculate ganglia were rapidly excised from CO_2-euthanized mice and placed in enzyme solution [minimum essential medium with Earle's balanced salts (MEM/EBSS; Hyclone) containing 1.25 mg/ml trypsin (Sigma-Aldrich) and 2.5 mg/ml collagenase A (Roche Diagnostics)] for 30 min. Digested ganglia were washed three times with MEM/EBSS before gentle trituration with a fire-polished glass pipette. Cells were resuspended in HEPES buffer containing the following (in mM): 136 NaCl, 5.6 KCl, 1 $MgCl_2$, 2.2 $CaCl_2$, 11 glucose, 10 HEPES; pH adjusted to 7.4 with NaOH before plating on poly-D-lysine (0.02 mg/ml; BD Bioscience) and laminin (0.02 mg/ml; Sigma-Aldrich)-coated coverslips.

Calcium imaging. Fura-2-AM (50 μM, Invitrogen) stock was prepared in HEPES buffer containing 2.5% DMSO and 0.01% Pluronic F-127 (Invitrogen) and then pipetted into the medium bathing the coverslips to a final concentration of 2 μM Fura-2-Am. Cells were loaded for 20 min before washing with HEPES buffer. The test compounds (all from Sigma-

Aldrich), ATP, 5-HT, m-chlorophenylbiguanide (CPG), ondansetron (ODS), and 55 mM KCl (with KCl replacing equimolar NaCl) were added to HEPES buffer. For experiments testing effects of pentobarbital on the ganglion cells, nembutal sodium solution (pentobarbital sodium; Oak Pharmaceuticals) was added to HEPES buffer at a final concentration of 150 or 800 μM. Fura-2-AM-loaded cells were imaged through a 40× oil-immersion objective lens of an inverted microscope and acquired with a Sensicam QE CCD camera (PCO-Tech). Emission at ~510 nm was collected from excitations at 350 and 380 nm. Images were collected every 3 s using Imaging Workbench 5 software (Indec Biosystems). Raw data are represented as change in fluorescence ratio normalized to baseline fluorescence ratio. Dose–response curves were fit with a four parameter logistic function using Sigmaplot (Systat Software; SciRes_000184).

Nerve recording. Two different anesthetics were tested in these experiments. Some mice were anesthetized with sodium pentobarbital, a common anesthetic used for taste nerve recording (Horio et al., 2011) and used in a recent study on the possible role of 5-HT_1 and 5-HT_3 in taste function (Jaber et al., 2014). Because barbiturate anesthetics are reported to interfere with functionality of 5-HT_3 receptors in several *in vitro* systems (Jenkins et al., 1996; Barann et al., 1997; Barann et al., 2000; Rüsch et al., 2007), we also tested urethane, which gave significantly different results (described below). Mice were anesthetized using injections of sodium pentobarbital (50 mg/kg, i.p.) or urethane (2 g/kg, i.p.; Sigma Chemical) and tracheotomized to facilitate breathing. The chorda tympani nerve was exposed using a ventral approach and cut near the tympanic bulla. The whole dissected nerve was placed on a silver electrode and a reference electrode was placed in the nearby tissue. Taste responses were amplified (P511; Grass Instruments), integrated (time constant 0.5 s) and collected using Acknowledge software (Biopac). The anterior tongue was stimulated with a continuous flow (Mini-pump; Fisher Scientific) and different tastants were injected into this flow: NH_4Cl 100 mM, sucrose 500 mM, NaCl 100 mM, monosodium glutamate (MSG) 300 mM with amiloride 100 μM, quinine 10 mM, citric acid (3, 5, 10, and 20 mM), and HCl (3, 5, 10, and 20 mM). The tastants were applied for 30 s and rinsed with water for 40 s. In some experiments, a specific antagonist of 5-HT_3 receptors (ODS dissolved in 0.9% NaCl; 1 mg/kg) or a vehicle control (0.9% NaCl) was injected intraperitoneally after all stimuli had been successively applied to the tongue. Fifteen minutes after the injection, the same stimuli were reapplied and responses compared before and after injection.

To analyze the data, the amplitude of the integrated responses was averaged for 30 s using Acknowledge software (Biopac) and normalized to the baseline (averaged for 5 s before each taste stimulation). We chose to normalize to the baseline activity as we have done in the past (Vandenbeuch et al., 2013) because serotonergic transmission could affect responses to most taste stimuli. Small drifts in baseline were observed over the course of the experiments, but these changes had little effect on the interpretation of the data because response magnitude was proportional to baseline activity. Individual mice with large drifts in baseline were excluded from analysis. The normalized responses then were compared using a two-way ANOVA with Tukey's *post hoc* test using Statistica software (verseion 10; Statsoft) for grouped tastants [3–20 mM citric acid, 3–20 mM HCl, and "others" (NH_4Cl, NaCl, sucrose, MSG with amiloride, and quinine)]. A statistical summary for nerve recording data is provided in Table 4.

Statistics. All data are represented as normalized raw data or as mean ± SEM. All statistical analyses were performed using Sigmaplot (Systat Software; SciRes_000184) or Statistica (version 10; Statsoft). $p < 0.05$ was considered statistically significant.

Table 4. Statistical comparisons for nerve-recording data

	Df	*F*	*p*
WT (7) vs KO (8) (urethane)			
Citric acid	52	5.22	0.017
HCl	39	3.29	0.009
Others	39	4.44	0.001
WT (6), pre vs post ODS injection (urethane)			
Citric acid	40	0.81	0.004
HCl	30	5.45	0.011
Others	30	2.14	0.525
WT (4), pre vs post NaCl injection (urethane)			
Citric acid	20	0.11	0.845
HCl	18	0.27	0.959
Others	18	0.12	0.979
WT (8) vs KO (7) (pentobarbital)			
Citric acid	39	2.09	0.240
HCl	39	1.89	0.147
Others	52	1.52	0.209
WT, urethane (7) vs pentobarbital (8)			
Citric acid	52	6.09	<0.001
HCl	39	6.74	<0.001
Others	39	10.19	<0.001
KO, urethane (8) vs pentobarbital (7)			
Citric acid	42	0.58	0.632
HCl	42	0.44	0.728
Others	56	3.78	0.008
WT, pentobarbital (8) vs post-ODS (6)			
Citric acid	36	2.30	0.094
HCl	26	0.73	0.540
Others	48	2.43	0.060

Degrees of freedom (*Df*), *F*-statistic, and *p*-values are for two-way ANOVAs comparing nerve recording data. Number of mice are in parentheses. For *post hoc* test results, see Figures 6 and 7. Citric acid and HCl, 3–20 mM. "Others," 100 mM NH_4Cl, 500 mM sucrose, 100 mM NaCl, 300 mM MSG plus 100 μM ammiloride, and 10 mM quinine.

Results

5-HT_{3A} mRNA is expressed in ganglion cells

RT-PCR shows 5-HT_{3A} transcripts in geniculate ganglia as well as in brain (Fig. 1*A*). Negative control experiments using the same primers on ganglia of 5-HT_{3A}KO mice show no detectable 5-HT_{3A} mRNA. *In situ* hybridization on sections of gustatory ganglia (geniculate, petrosal/nodose) and a somatosensory ganglion (trigeminal) were performed to reveal serotonin receptor gene expression at the cellular level. In all cases, a subset of ganglion cells displayed robust label for 5-HT_{3A} mRNA (Fig. 1*B*–*G*).

5-HT_{3A}-driven GFP is expressed in a subset of geniculate ganglion cells innervating the tongue and intragemmal fibers of taste buds

To first determine whether gustatory afferents express GFP in 5-HT_{3A}GFP mice, we examined the geniculate ganglion and taste buds. Similar to the results from *in situ* hybridization, a subset of geniculate ganglion cells displayed bright GFP fluorescence (Fig. 2*A*). Because all taste fibers express the $P2X_3$ purinergic receptor (Ishida et al., 2009; Vandenbeuch et al., 2015), we immunoreacted geniculate ganglion sections from 5-HT_{3A}GFP mice with antibodies against GFP (to amplify 5-HT_{3A}GFP signal) and against $P2X_3$. GFP immunoreactivity was detected in a subset of geniculate ganglion neurons (169/682, 24.8%; Fig. 2*B*,*C*), whereas the $P2X_3$ signal was present in nearly all ganglion cells (664/682, 97.4%; Fig. 2*B*,*C*).

To determine whether any 5-HT_{3A}GFP-positive ganglion cells of the geniculate ganglion innervate taste buds, as opposed to the external ear, we injected the retrograde tracer FluoroGold into the anterior tongue and palatal taste fields. After 5 d, many cells in the geniculate ganglion were labeled with FluoroGold. Semiquantitative analysis revealed that approximately half (73/138) of FluoroGold-labeled cell bodies exhibited GFP label, whereas in the ganglion as a whole, including both gustatory and nongustatory innervation, a significantly lower proportion of ganglion cells exhibit GFP fluorescence [139/468; $\chi^2(1,n = 606) = 25.21$, $p < 0.0001$ Pearson's χ^2 test; Fig. 2*D*–*G*]. Therefore, GFP-expressing ganglion cells preferentially innervate taste buds.

Consistent with GFP expression in the geniculate ganglion, most taste buds innervated by the geniculate ganglion contained some GFP-labeled intragemmal nerve fibers. The GFP-expressing nerve fibers often were closely associated with serotonergic type III cells (Fig. 3*A–D*), suggesting the possibility of serotonergic transmission between serotonergic type III taste cells and 5-HT$_{3A}$GFP-expressing nerve fibers. 5-HT$_{3A}$-driven GFP was not expressed in taste receptor cells. These GFP-labeled fibers were, however, only a subset of the total gustatory innervation of the taste buds, as revealed by immunoreactivity for P2X$_3$ (Fig. 3*E*).

Geniculate ganglion neurons expressing 5-HT$_{3A}$-driven GFP have functional 5-HT$_3$ receptors

We next tested the responsiveness of GFP-expressing and GFP-nonexpressing geniculate ganglion neurons to exogenously applied 5-HT. Ganglion cells were isolated from 5-HT$_{3A}$GFP mice and loaded with the membrane-permeable, ratiometric calcium indicator dye Fura-2-AM. We identified "healthy" cells by a response to 10 μM ATP because all geniculate ganglion neurons express P2X-type purinergic receptors (Ishida et al., 2009; Vandenbeuch et al., 2015). We observed similar robust increases of intracellular calcium concentrations in response to KCl and ATP in both GFP-expressing ($n = 28$) and GFP-nonexpressing cells ($n = 12$), whereas 5-HT elicited an increase in intracellular calcium only in GFP-expressing cells (KCl: $t_{(40)} = 0.98$, $p = 0.33$; ATP $t_{(38)} = 1.04$, $p = 0.30$; 5-HT: $t_{(38)} = 5.24$, $p < 0.0001$ Student's t tests; Fig. 4*A*,*B*,*F*). In GFP-expressing cells, dose–response curves revealed EC_{50} values of 1.2 ± 0.1 μM ($n = 9$) for ATP and 1.5 ± 0.3 μM ($n = 5$) for 5-HT (Fig. 4*E*). Next, to test whether the response to 5-HT was specific to 5-HT$_3$ receptors, we blocked 5-HT$_3$ receptors with ODS and coapplied 5-HT. Preapplication of 1 μM ODS blocked the response to 5-HT ($n = 12$, $t_{(11)} = 7.09$, $p < 0.0001$ paired Student's t test), but not to ATP ($n = 6$, $t_{(5)} = 0.66$, $p = 0.55$ paired Student's t test; Fig. 4*C*,*G*,*H*). In most cases, the antagonistic effects of ODS were reversible. The ability of the specific 5-HT$_3$ antagonist to block Ca^{2+} responses indicates that 5-HT$_3$ is the only 5-HT receptor capable of generating a Ca^{2+} signal in the ganglion cells. As an alternative test for receptor specificity, we applied the 5-HT$_3$ receptor agonist CPG, which induced an increase in intracellular calcium in 5-HT$_{3A}$GFP cells; the agonistic

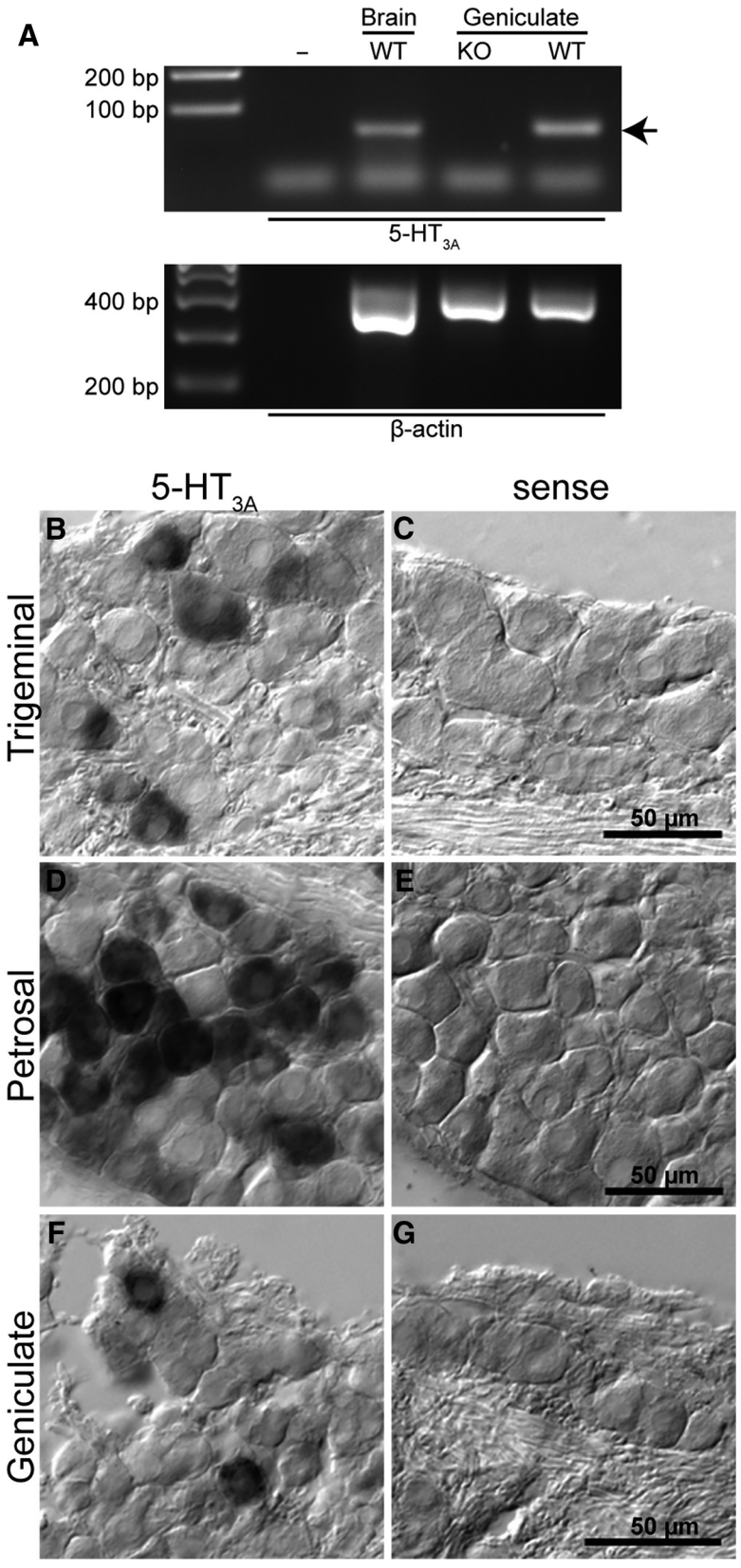

Figure 1. Expression of 5-HT$_{3A}$ mRNA in geniculate ganglia as demonstrated by RT-PCR and *in situ* hybridization. ***A***, RT-PCR showing the presence of 5-HT$_{3A}$ transcripts in brain and geniculate ganglion of WT mice, but the lack of 5-HT$_{3A}$ mRNA in geniculate ganglion of 5-HT$_{3A}$KO mice. Arrow indicates expected size of 66 bp 5-HT$_{3A}$ band. Primer dimers likely constitute the smallest band seen in both control and experimental lanes. PCR of β-actin was used as a loading control (lower gel). ***B–G,*** *In situ* hybridization for 5-HT$_{3A}$ in three cranial ganglia and the respective sense controls. ***B***, ***C***, Trigeminal ganglion. ***D, E,*** Petrosal ganglion. ***F, G,*** Geniculate ganglion. In each ganglion, a subpopulation of ganglion cells show robust signal for 5-HT$_{3A}$ mRNA.

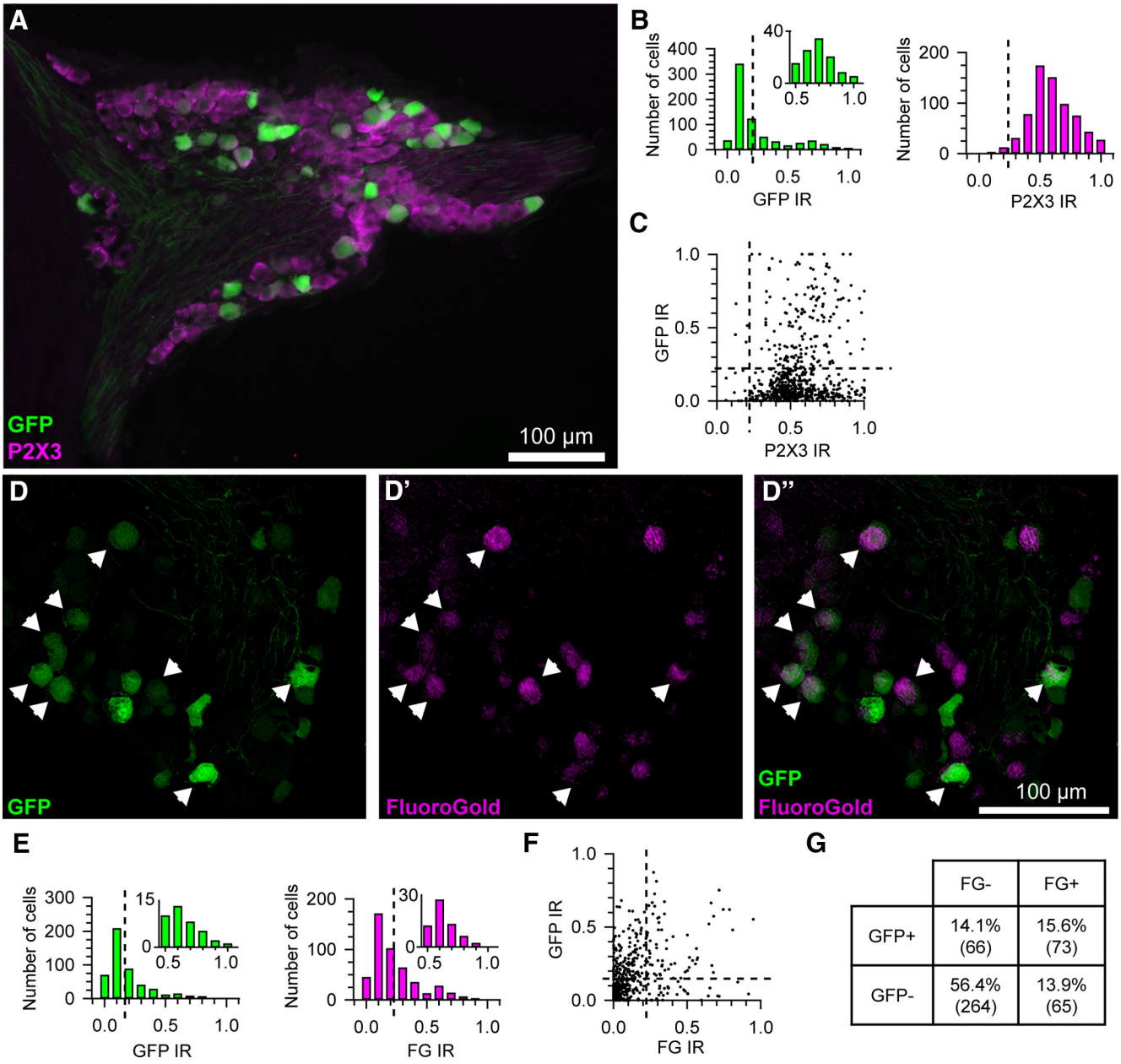

Figure 2. 5-HT_{3A}-driven GFP is expressed in geniculate ganglion neurons that innervate the tongue. ***A***, Confocal *Z*-projection of 10 0.7 μm optical slices of geniculate ganglion from a 5-HT_{3A}GFP mouse showing expression of GFP (green) and $P2X_3$ (magenta). Scale bar, 100 μm. ***B***, Histograms of GFP and $P2X_3$ normalized immunoreactivity of individual cells showing that whereas the $P2X_3$ staining shows a unimodal normal distribution (mean 0.58), the GFP population is bimodal suggestive of high-expressing (mean = 0.69) and low- or nonexpressing populations (mean 0.12). Insert at upper right shows the higher expressing population rescaled along the abscissa. ***C***, Scatterplot comparing relative fluorescence intensity for normalized $P2X_3$ and GFP immunoreactivity. No correlation exists between the two factors ($r = 0.16$, Pearson's correlation; $n = 5$ mice, 9 ganglia, 682 cells). Dotted lines (***B***, ***C***) indicated threshold for each channel. ***D***, Confocal *Z*-projections of geniculate ganglion from 5-HT_{3A}GFP mice 5 d after FluoroGold injection showing expression of GFP (green) and FluoroGold label (FG; magenta). Arrows indicate double-labeled cells (above threshold in each channel). ***E***, Histograms of GFP and FG normalized fluorescence intensity of individual cells showing bimodal distributions suggestive of a high-expressing population (mean GFP: 0.59, FG: 0.62) and a nonexpressing population (mean GFP: 0.08, FG: 0.08). ***F***, Scatterplot comparing the relative fluorescence intensity for normalized GFP and FG fluorescence. No correlation exists between the two factors ($r = 0.35$ Pearson's correlation; $n = 3$ mice, 6 ganglia, 468 cells). Dotted lines (***E***, ***F***) indicate threshold for each channel. ***G***, Table showing relative number of cells showing suprathreshold expression of GFP and FG label.

effect was blocked by ODS ($n = 5$, $t_{(4)} = 20.55$, $p < 0.0001$ paired Student's *t* test; Fig. 4*D*,*H*). From these data, we conclude that activation of geniculate ganglion neurons by 5-HT, as measured by cytosolic Ca^{2+}, is mediated only by 5-HT_3 receptors.

Ganglion cell responses to 5-HT are lacking in 5-HT_{3A}KO mice

Our data demonstrate that a subset of geniculate ganglion neurons expresses 5-HT_3 receptors and innervates taste buds, including serotonergic type III cells. These findings suggest that 5-HT released from type III taste cells might activate gustatory sensory terminals in taste buds. Given these conditions, we hypothesized that 5-HT_3 receptors would be implicated in the transmission of type III cell-mediated taste information from taste buds to the nerve fibers. To test this, we used mice lacking functional 5-HT_3 receptors (5-HT_{3A}KO mice). Successful genetic deletion of 5-HT_3 was confirmed by RT-PCR (Fig. 1*A*). In addition, we tested whether other 5-HT receptors were upregulated after ge-

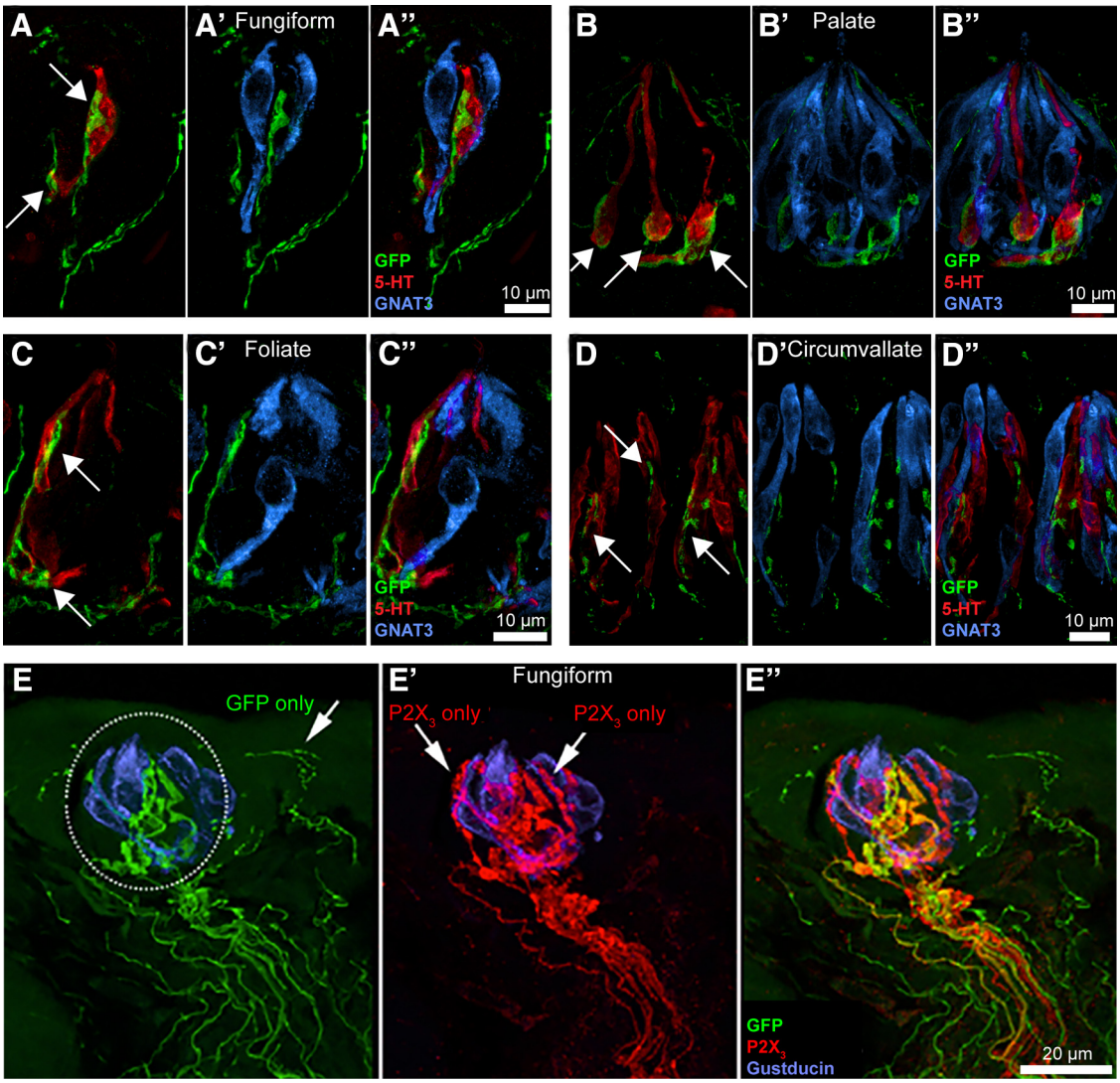

Figure 3. 5-HT_{3A}-driven GFP is expressed in a subset of nerve fibers innervating taste buds. ***A–D,*** Confocal *Z*-projections of taste buds of a 5-HT_{3A}GFP mouse showing expression of GFP (green), 5-HT (serotonin, type III taste cell marker, red), and GNAT3 (gustducin, type II taste cell marker; blue). The GFP-labeled fibers are closely associated with 5-HT labeled type III cells (white arrows) in all taste fields. ***A***, Eight 0.7 μm optical slices of a taste bud from a fungiform papilla. ***B***, Thirteen 0.7 μm optical slices of a palatal taste bud. ***C***, Ten 0.7 μm optical slices of a taste bud from a foliate papilla. ***D***, Eleven 0.7 μm optical slices of a taste bud from a circumvallate papilla. Arrows highlight sites of convergence between 5-HT-expressing type III cells and 5-HT_{3A}GFP-expressing nerve fibers. Scale bars, 10 μm. ***E***, Longitudinal section through a fungiform papilla from a 5-HT_{3A}GFP mouse stained for $P2X_3$ (red) and gustducin (blue). Intragemmal (inside the taste bud) taste fibers are stained with the $P2X_3$ antibody, whereas GFP expression occurs in a subset of the intragemmal fibers as well as perigemmal fibers innervating the surrounding epithelium. The perigemmal fibers (GFP-only in ***E***), presumably of trigeminal origin, exhibit only 5-HT_{3A}-driven GFP, whereas intragemmal GFP-labeled fibers are also immunoreactive for $P2X_3$. Some intragemmal fibers only show $P2X_3$ immunoreactivity (arrows in ***E'***). Confocal *Z*-stack 9.6 μm. Off-tissue noise was removed digitally. Blue hues were modified using Adobe Photoshop to enhance visibility.

netic deletion of 5-HT_3 by measuring 5-HT responses in isolated geniculate ganglion neurons of WT and 5-HT_{3A}KO mice. Approximately 25% of all WT geniculate neurons (5/19; Fig. 5) responded to exogenous 5-HT with an increase in intracellular calcium, whereas no neurons from 5-HT_{3A}KO mice responded (0/25, $p = 0.011$, Fisher's exact test; Fig. 5). Therefore, even after genetic elimination of the 5-HT_3 receptor, no other serotonin receptors were capable of generating a calcium signal in the ganglion cells.

Contribution of 5-HT_3 receptors to transmission of taste information

Under urethane anesthesia, the chorda tympani nerves of both WT and KO animals responded robustly to all classes of taste stimuli. Nonetheless, responses in KO animals to most stimuli (100 mM NH_4Cl, 500 mM sucrose, 300 mM MSG with amiloride, 5–20 mM citric acid, and 5–20 mM HCl) were reduced compared with WT (Fig. 6*B*, Table 4), suggesting a role for 5-HT_3 signaling in more than just acid and salt transmission; that is, tastants likely to evoke direct type III cell-mediated signaling.

To further examine the role of 5-HT_3 receptors in taste transmission, we tested whether the specific 5-HT_3 antagonist ODS decreased taste responses in WT mice under urethane anesthesia. Intraperitoneal injection of ODS significantly decreased chorda tympani nerve response magnitude to acids (sour tastants), as well as NaCl (Fig. 6*C*, Table 4). Injection of vehicle had no effect on the magnitude of any responses, indicating that reductions measured with ODS were not the result of general loss of nerve activity over the course of the experiment (Fig. 6*D*, Table 4). Although the effects of ODS on acid and salt responses closely phenocopied 5-HT_{3A}KO, the effects of ODS on other stimuli were less robust but trended in the same direction.

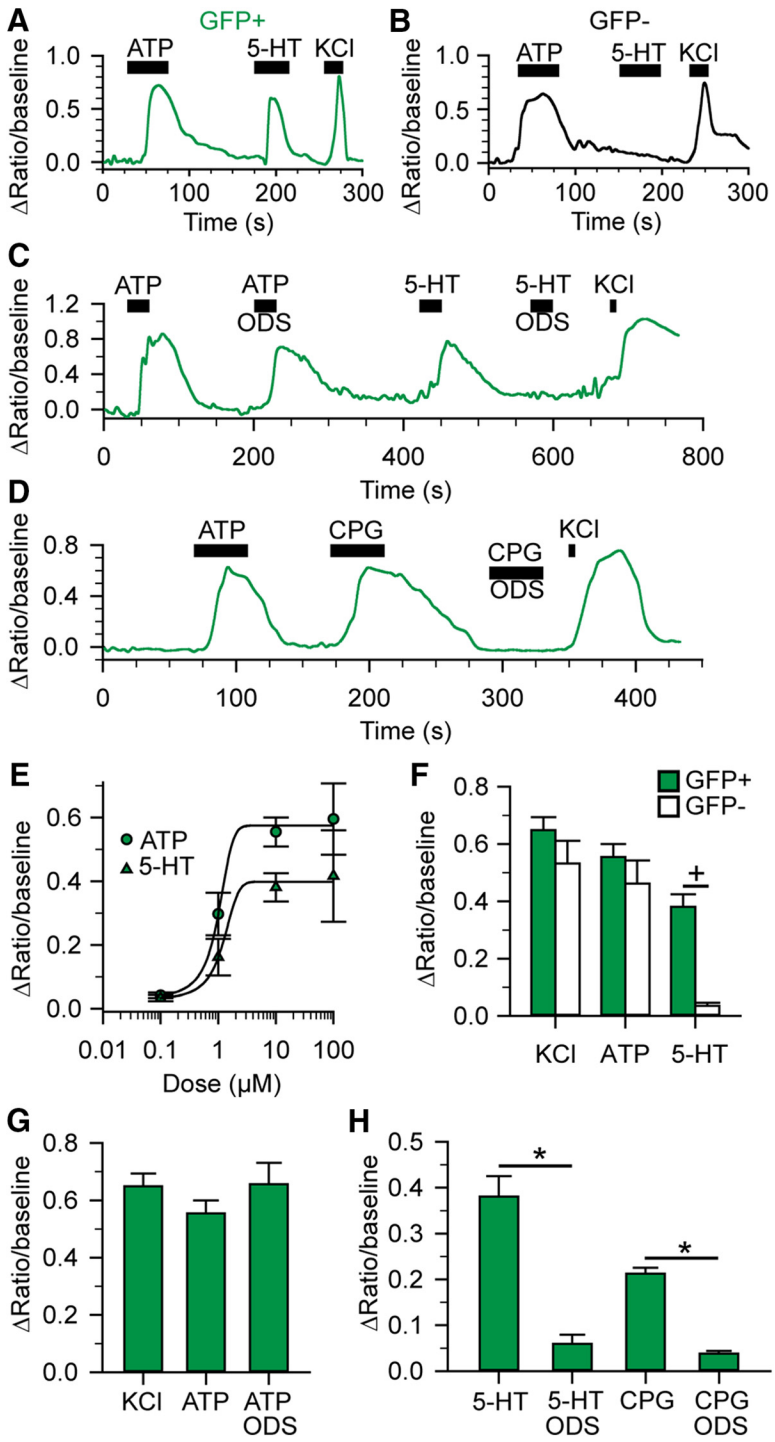

Figure 4. 5-HT_{3A}GFP-expressing cells show increased intracellular Ca^{2+} in response to 5-HT_3 activation. ***A, B,*** Ca^{2+} signals from GFP^+ (***A***) and GFP^- (***B***) geniculate ganglion cells in response to 10 μM ATP, 10 μM 5-HT, and 55 mM KCl. ***C, D***, Ca^{2+} signals from GFP+ geniculate ganglion cells in response to 10 μM ATP, 10 μM ATP + 1 μM ODS, 10 μM 5-HT, 10 μM 5-HT + 1 μM ODS, and 55 mM KCl (***C***) or 10 μM ATP, 10 μM CPG, 10 μM CPG + 1 μM ODS, and 55 mM KCl (***D***). ***E***, ATP (circles) and 5-HT (triangles) dose–response curves for 5-HT_{3A}GFP-expressing geniculate ganglion cells. ***F***, Average responses to KCl, ATP, and 5-HT in GFP^+ and GFP^- ganglion cells. Cross indicates $p < 0.05$, Student's *t* test. ***G***, Average responses of 5-HT_{3A}GFP-expressing cells to 55 mM KCl, 10 μM ATP and ATP + 1 μM ODS. All conditions were measured in each cell ($n = 5$, $p = 0.399$, one-way ANOVA). ***H***, Average responses of 5-HT_{3A}GFP-expressing cells. Responses to both 5-HT and CPG are blocked by the 5-HT_3-antagonist ODS. Asterisks indicate $p < 0.0001$, paired Student's *t* tests.

Effects of anesthesia on 5-HT_{3A} signaling

We find that pharmacological blockade of 5-HT_3 receptors with ODS, similar to the 5-HT_3KO, significantly reduces chorda tympani responses to multiple stimuli, including acids and salt. In contrast, Jaber et al. (2014), using pentobarbital anesthetic, reported that ODS injection in rats had no effect on chorda tympani responses. Because barbiturate anesthetics (e.g., pentobarbital) are reported to block 5-HT_3 signaling in heterologous expression systems (Barann et al., 2000; Rüsch et al., 2007), we tested the effects of different anesthetics (pentobarbital vs urethane) on chorda tympani responses. Similar to the findings reported by Jaber et al. (2014) for rats, chorda tympani responses to all tastants were similar for WT and KO mice under pentobarbital anesthesia (Fig. 7*A*, Table 4). Next, we compared the difference between urethane and pentobarbital anesthesia in WT mice. In WT animals, responses to all tastants except 5 mM quinine were larger under urethane anesthesia than with pentobarbital (Fig. 7*B*, Table 4), but this difference in response magnitude with anesthetic did not occur in the KO mice (Fig. 7*C*, Table 4), with the exception of sucrose. The lack of effect of pentobarbital in 5-HT_3KO mice suggests an interaction between the drug and 5-HT_3 receptors *in vivo*. To further understand the mechanism by which pentobarbital affects chorda tympani responses, we applied pentobarbital to isolated 5-HT_{3A}GFP-expressing geniculate ganglion neurons. Similar to other *in vitro* studies (Barann et al., 1997; Barann et al., 2000; Rüsch et al., 2007), pentobarbital inhibited 5-HT induced calcium responses in geniculate ganglion neurons [$n = 10$ cells ($n = 5$ for 150 μM pentobarbital), $F_{(1,24)} = 105.66$, $p < 0.001$ one-way repeated-measures ANOVA; Figure 7*D*,*E*]. The block of serotonin signaling in ganglion cells by pentobarbital could explain the reduced chorda tympani responses in WT mice under pentobarbital anesthesia (Fig. 7*B*).

In summary, both genetic deletion and pharmacological blockade of the 5-HT_3 receptor affect transmission of multiple taste modalities. Neither manipulation of 5-HT_3 entirely eliminates the responses, suggesting that other neurotransmitters such as ATP participate in neurotransmission in this system.

Discussion

Taste stimuli activate taste receptor cells, which release one or more neurotransmitters to excite gustatory afferent nerve fibers (Roper, 2013). These nerve fibers encode taste quality information, which is transmitted to the brainstem gustatory complex. However, a paucity of information exists on the steps between taste receptor cell activation and afferent nerve fiber firing. Although ATP acting on

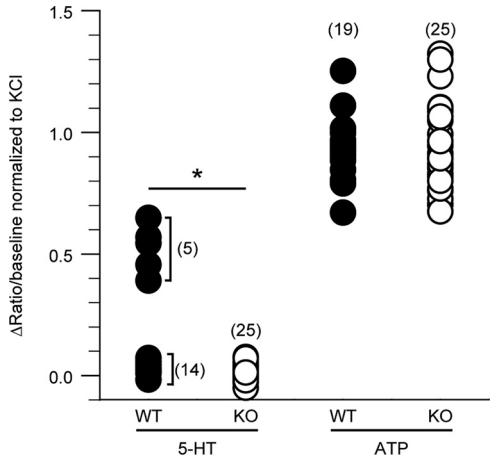

Figure 5. Geniculate ganglion neurons of 5-HT_{3A}KO mice do not respond to serotonin. Normalized responses of Fura-2-AM loaded geniculate ganglion neurons revealed that a subset (solid circles; 5/19) of WT neurons were activated by 10 μM 5-HT; no neurons from 5-HT_{3A}KO animals (open circles; 0/25) responded to 5-HT, yet all responded to 10 μM ATP and 55 mM KCl. Symbols represent individual cells. Data are normalized to the response to KCl. Asterisk indicates $p < 0.05$, Fisher's exact test.

neural P2X receptors is crucial for transmission of all taste qualities (Finger et al., 2005; Vandenbeuch et al., 2015), the role of other substances acting as neurotransmitters, cotransmitters, or modulators of neural activity is less clear (Kaya et al., 2004; Huang et al., 2005; Jaber et al., 2014; Takai et al., 2015). Further, whereas ATP release from type II taste cells has been observed in response to bitter-, sweet-, and umami-tasting stimuli, ATP release has not been detected from type III taste cells (Huang et al., 2007; Romanov et al., 2007; Murata et al., 2010). These data suggest that one or more other transmitters may play a role in afferent signaling. In the present study, we have investigated the role of 5-HT in the communication between taste receptor cells and afferent nerve fibers.

Using a mouse expressing GFP under the control of the 5-HT_{3A} promoter, we found that a subset of geniculate ganglion neurons innervating taste buds expresses GFP, suggesting the presence of 5-HT_3 receptors. Our physiological analysis established that functional 5-HT_3 receptors are present only in these GFP-labeled ganglion cells and that 5-HT_3 is required for ganglion cell responses to 5-HT. Although other 5-HT receptors may exist in the ganglion, 5-HT_3 is the only ionotropic 5-HT receptor and is normally involved in excitatory signaling in the nervous system (Galligan et al., 2000; Galligan, 2002). Further, in the absence of 5-HT_3 signaling, ganglion cells do not respond to 5-HT, as assessed by Ca^{2+} imaging. It is possible that the 5-HT_3 receptor that we demonstrate in the ganglion cell somata is not transported to the distal processes that innervate taste buds but other receptors present in cell bodies of taste ganglia are, including P2X receptors (Bo et al., 1999) and GLP-1 receptors (Shin et al., 2008). Furthermore, injection of 5-HT_3 antagonist *in vivo* materially affects taste responses recorded from the afferent nerves distal to the ganglion, suggesting a peripheral site of action.

Although 5-HT_3 receptors play a role in afferent signaling in taste buds, the full neural taste response clearly involves other neurotransmitter receptors. ATP acting on $P2X_2$ and $P2X_3$ receptors is required for transmission of all taste qualities (Finger et al., 2005; Vandenbeuch et al., 2015). The source of ATP for transmission of bitter, sweet, and umami tastants is evidently the type II taste cells, which release ATP with gustatory activation (Huang et al., 2007; Murata et al., 2010). For acids, the taste of which is mediated by type III cells, one possibility is that ATP is coreleased from vesicles along with 5-HT. However, type III cells do not express the vesicular nucleotide transporter VNUT, which is reportedly required to load ATP into vesicles (Iwatsuki et al., 2009), and ATP release has not been detected from type III cells, so the source of ATP with sour stimulation is unclear (Huang et al., 2007; Romanov et al., 2007). One possibility is that tonic release of ATP, possibly from type II cells or nongustatory tissue, may be required to set a basal tone of afferent nerve depolarization upon which another type III cell transmitter such as 5-HT provides additional depolarization to excite gustatory afferents in response to acids. In the absence of basal P2X activation, the gustatory afferents may simply be too hyperpolarized to permit generation of action potentials by other transmitters and modulators. Nonetheless, the persistence of residual taste-induced neural activity in the absence of 5-HT_3 signaling strongly suggests that ATP, possibly along with other neurotransmitters, provides sufficient signaling to generate a neural response to taste.

A role for 5-HT in taste signaling has been described in humans in that 5-HT reuptake inhibitors decrease the threshold for quinine and sucrose (Heath et al., 2006), but whether this may be a peripheral or central effect is unclear. In rats, however, the same 5-HT reuptake inhibitors had no effect on the behavioral taste thresholds to sucrose, NaCl, or citric acid, thus confounding the role of 5-HT in peripheral taste signaling (Mathes and Spector, 2014). Whether these confounds represent differences in methodology or possibly species differences remains to be determined.

In taste buds, 5-HT is synthesized, stored, and ultimately released by type III taste cells that respond to acidification (Huang et al., 2009, 2011) or high levels of NaCl (Oka et al., 2013). The serotonergic type III taste cells appear to contact the 5-HT_{3A}GFP-expressing taste nerve fibers, which then are positioned appropriately to respond to a 5-HT signal. Whole taste nerve recordings in WT mice show that 5-HT_3 antagonists (both ODS and pentobarbital) significantly decrease responses to most tastants, suggesting that 5-HT_3 receptors have a role in communication between taste receptor cells and afferent nerve fibers. Superficially, our findings seem discrepant with the lack of effect of intravascular injection of ODS on chorda tympani taste responses in rats (Jaber et al., 2014), but this apparent discrepancy is likely due to the use of barbiturate anesthetics in that study, which by itself in our experiments in mice blocks 5-HT_3 signaling.

The pronounced effect of barbiturate anesthetics on 5-HT_3 function as reported in our study *in vivo* mirrors previous findings in heterologous, *in vitro* systems (Jenkins et al., 1996; Barann et al., 1997; Barann et al., 2000; Rüsch et al., 2007), in which barbiturates act via an allosteric interaction with the receptor (Davies, 2011). In our study, pentobarbital inhibited 5-HT evoked calcium signals in geniculate ganglion neurons and, at anesthetic levels in mice, significantly inhibits 5-HT_3 function *in vivo*. For the anesthetic doses used in our experiments, plasma and tissue concentrations of intraperitoneally injected pentobarbital in mice are likely to be at or above the reported IC_{50} values for 5-HT_3 receptors (Nelson and Halberg, 1973). Other investigators working with human 5-HT_{3A} suggest that barbiturates only affect these receptors at doses considerably higher than the anesthesic levels used in our study (Rüsch et al., 2007).

We note that the effects of blocking 5-HT_3 or knocking out 5-HT_{3A} were not restricted to established type III cell-mediated modalities—that is, acids (Huang et al., 2008) and high concentrations of NaCl (Oka et al., 2013)—but also affected responses to other tastants, including NH_4Cl and sucrose. Although the cell

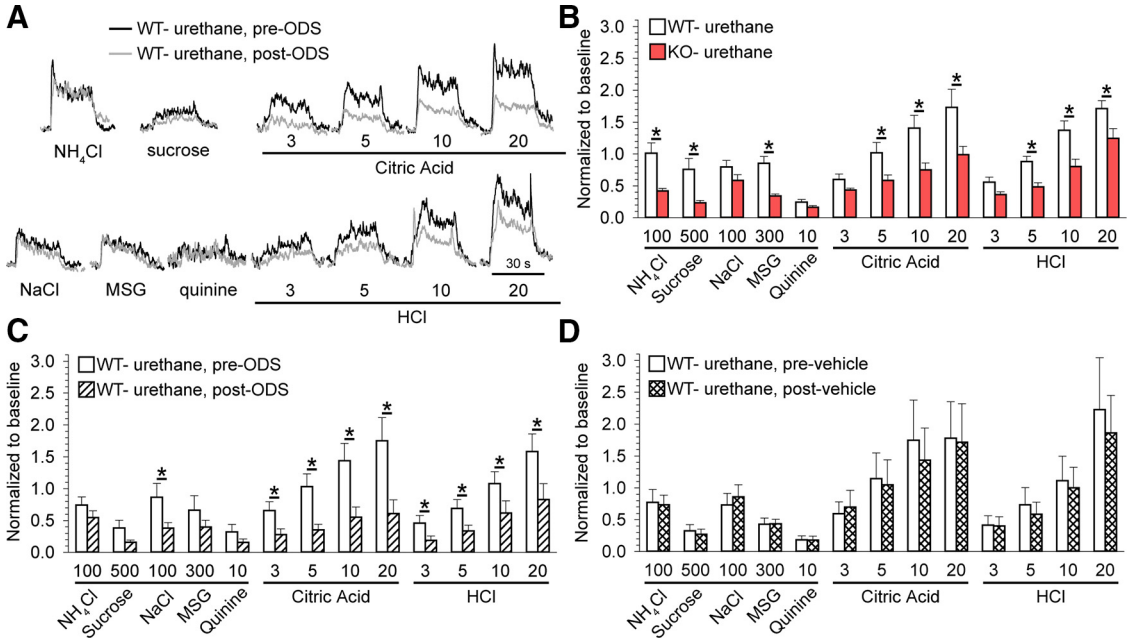

Figure 6. Role of 5-HT_{3A} signaling in taste transmission. ***A,*** Example of integrated chorda tympani responses of a single WT mouse under urethane anesthesia to multiple stimuli before and after ODS injection (1 mg/kg, i.p). Scale bar, 30 s. ***B***, Average chorda tympani responses normalized to baseline of WT and 5-HT_{3A}KO mice. Responses to multiple stimuli were significantly larger in WT mice. $n = 7$ WT mice (6–7 trials per tastant), 8 KO mice (6–8 trials per tastant). ***C, D***, Average chorda tympani responses in WT mice before and after injection of the 5-HT_3 antagonist ODS (***C***) or vehicle (***D***). The responses to acids were significantly smaller after ODS treatment, but not vehicle injection. $n = 6$ mice (6 trials per tastants) ODS, 4 mice (4 trials per tastants) vehicle. Data are presented as mean ± SEM. Asterisks indicate $p < 0.05$, two-way ANOVA with Tukey's *post hoc* test.

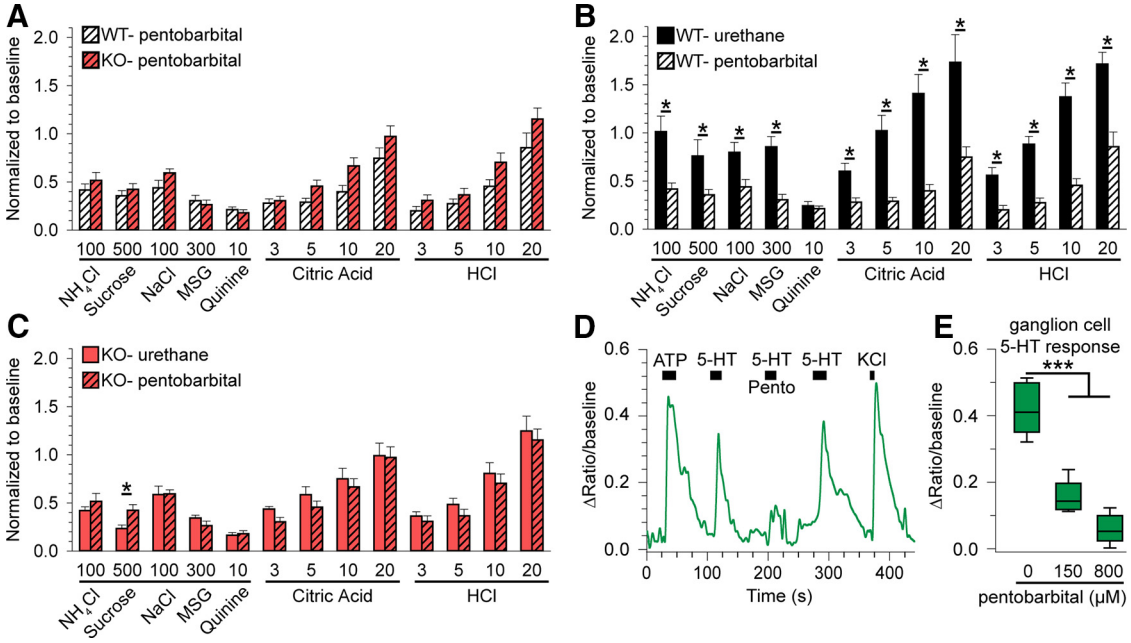

Figure 7. Effect of pentobarbital anesthesia on 5-HT_{3A} signaling. ***A,*** Average chorda tympani responses of WT and 5-HT_{3A}KO mice under pentobarbital anesthesia. Responses to all stimuli were similar between WT and KO mice. $n = 8$ WT mice (7–8 trials per tastant), 7 KO mice (6–7 trials per tastant). ***B***, Average chorda tympani responses of WT mice under different anesthetic conditions. Responses to most stimuli were significantly larger under urethane anesthesia. $n = 7$ mice urethane (6–7 trials per tastant), 8 mice pentobarbital (7–8 trials per tastant). ***C***, Average chorda tympani responses of 5-HT_{3A}KO mice under different anesthetic conditions. There was no significant difference in response to acid between pentobarbital and urethane anesthesia. The response to sucrose was significantly different under urethane anesthesia. $n = 8$ mice (7–8 trials per tastant) for urethane, 7 mice (6–7 trials per tastants) for pentobarbital. ***D***, Example Fura-2-loaded geniculate ganglion neuron response to 10 μM ATP, 10 μM 5-HT, 10 μM 5-HT + 800 μM pentobarbital, and 55 mM KCl. ***E***, Summary data of all ganglion cells in response to 5-HT and 5-HT + pentobarbital. $n = 10$ cells for 0 and 800 μM pentobarbital, $n = 5$ cells 150 μM pentobarbital. Nerve-recording summary data are presented as mean ± SEM. Asterisks indicate $p < 0.05$, two-way ANOVA with Tukey's *post hoc* test. Triple asterisks indicate $p < 0.001$, one-way repeated-measures ANOVA with Tukey's *post hoc* test.

type mediating NH_4Cl responses is unclear, nonserotonergic, type II taste cells are responsible for transmission of sucrose. The unexpected involvement of 5-HT_3 in sucrose responses may be attributable to the secondary release of 5-HT from type III cells in response to the ATP released from type II taste cells during stimulation with sweeteners (Meredith et al., 2015). In lingual slices, type III cells show intracellular calcium responses to multiple stimuli, including sweeteners (Tomchik et al., 2007), likely due to secondary activation via sweet-responsive type II cells. The 5-HT thus released has been hypothesized to be involved in a negative feedback onto type II cells via 5-HT_{1A} receptors (Huang et al., 2009). Nonetheless, some of the released 5-HT will likely activate the neural 5-HT_3 receptors. If a significant stimulation of 5-HT_3 expressing afferents occurs with sweet tastant stimulation, then one would expect sweet-tasting stimuli to evoke indirect side band excitation of sour-best afferent fibers. This has not been observed in single-fiber studies of taste specificity in mice (Ninomiya et al., 1982, 1984a,b); however, those studies were performed using pentobarbital as an anesthetic, so the 5-HT_3 receptors would have been blocked under those conditions.

The widespread use of pentobarbital as an anesthetic in studies entailing peripheral nerve recordings (Ninomiya et al., 1982; Dahl et al., 1997; Nelson et al., 2002; Horio et al., 2011; Oka et al., 2013; Jaber et al., 2014; Vandenbeuch et al., 2015; Barretto et al., 2015) calls into question the degree to which these studies reflect the native condition of the system. Because type III cells appear to integrate information from other receptor cells (Tomchik et al., 2007) and use the 5-HT_3 system to transmit information, these previous nerve recording studies may have inhibited transmission of integrated cross-modal information from type III cells, leading to the appearance of strict labeled-line, modality-specific transmission of information. Interestingly, when nonbarbiturate anesthetics are used, a concentration-dependent increase in sideband excitation is observed in a subset of geniculate ganglion neurons (Wu et al., 2015). Perhaps this sideband excitation is due to intrabud signaling from type II to type III cells, thus increasing serotonin release and activation of 5-HT_3 receptors with increased stimulus concentration.

In summary, our results show that serotonin, released by taste buds and activating neural 5-HT_3 receptors, plays a significant but nonessential role in transmission of taste information from the tongue to the nervous system. Further, we show that pentobarbital and possibly other barbiturate anesthetics inhibit 5-HT_3-mediated responses in this system, affecting some taste modalities more than others. Because the large majority of recordings from taste nerves in the past have relied on such anesthetics, reexamination of single-fiber specificity in the system should be undertaken with nonbarbiturate anesthetics.

References

Banik Soma SR, Berdougo E, Doranz BJ (2011) Antibodies against membrane protein targets. Genet Eng Biotechnol News 31:18.

Barann M, Göthert M, Bönisch H, Dybek A, Urban BW (1997) 5-HT3 receptors in outside-out patches of N1E-115 neuroblastoma cells: basic properties and effects of pentobarbital. Neuropharmacology 36:655–664. CrossRef Medline

Barann M, Meder W, Dorner Z, Brüss M, Bönisch H, Göthert M, Urban BW (2000) Recombinant human 5-HT3A receptors in outside-out patches of HEK 293 cells: basic properties and barbiturate effects. Naunyn Schmiedebergs Arch Pharmacol 362:255–265. CrossRef Medline

Barretto RP, Gillis-Smith S, Chandrashekar J, Yarmolinsky DA, Schnitzer MJ, Ryba NJ, Zuker CS (2015) The neural representation of taste quality at the periphery. Nature 517:373–376. Medline

Bo X, Alavi A, Xiang Z, Oglesby I, Ford A, Burnstock G (1999) Localization of ATP-gated P2X2 and P2X3 receptor immunoreactive nerves in rat taste buds. Neuroreport 10:1107–1111. CrossRef Medline

Dahl M, Erickson RP, Simon SA (1997) Neural responses to bitter compounds in rats. Brain Res 756:22–34. CrossRef Medline

Davies PA (2011) Allosteric modulation of the 5-HT3 receptor. Curr Opin Pharmacol 11:75–80. CrossRef Medline

DeFazio RA, Dvoryanchikov G, Maruyama Y, Kim JW, Pereira E, Roper SD, Chaudhari N (2006) Separate populations of receptor cells and presynaptic cells in mouse taste buds. J Neurosci 26:3971–3980. CrossRef Medline

Dvoryanchikov G, Tomchik SM, Chaudhari N (2007) Biogenic amine synthesis and uptake in rodent taste buds. J Comp Neurol 505:302–313. CrossRef Medline

Finger TE, Danilova V, Barrows J, Bartel DL, Vigers AJ, Stone L, Hellekant G, Kinnamon SC (2005) ATP signaling is crucial for communication from taste buds to gustatory nerves. Science 310:1495–1499. CrossRef Medline

Foley JO, DuBois FS (1943) An experimental study of the facial nerve. J Comp Neurol 79:79–105. CrossRef

Fujimoto S, Ueda H, Kagawa H (1987) Immunocytochemistry on the localization of 5-hydroxytryptamine in monkey and rabbit taste buds. Acta Anat (Basel) 128:80–83. CrossRef

Galligan JJ (2002) Pharmacology of synaptic transmission in the enteric nervous system. Curr Opin Pharmacol 2:623–629. CrossRef Medline

Galligan JJ, LePard KJ, Schneider DA, Zhou X (2000) Multiple mechanisms of fast excitatory synaptic transmission in the enteric nervous system. J Auton Nerv Syst 81:97–103. CrossRef Medline

Hassaine G, Deluz C, Grasso L, Wyss R, Tol MB, Hovius R, Graff A, Stahlberg H, Tomizaki T, Desmyter A, Moreau C, Li XD, Poitevin F, Vogel H, Nury H (2014) X-ray structure of the mouse serotonin 5-HT3 receptor. Nature 512:276–281. CrossRef Medline

Heath TP, Melichar JK, Nutt DJ, Donaldson LF (2006) Human taste thresholds are modulated by serotonin and noradrenaline. J Neurosci 26:12664–12671. CrossRef Medline

Herness MS, Chen Y (2000) Serotonergic agonists inhibit calcium-activated potassium and voltage-dependent sodium currents in rat taste receptor cells. J Membr Biol 173:127–138. CrossRef Medline

Horio N, Yoshida R, Yasumatsu K, Yanagawa Y, Ishimaru Y, Matsunami H, Ninomiya Y (2011) Sour taste responses in mice lacking PKD channels. PLoS One 6:e20007. CrossRef Medline

Hoyer D, Schoeffter P (1991) 5-HT receptors: subtypes and second messengers. J Recept Signal Transduct 11:197–214. CrossRef

Huang AL, Chen X, Hoon MA, Chandrashekar J, Guo W, Tränkner D, Ryba NJ, Zuker CS (2006) The cells and logic for mammalian sour taste detection. Nature 442:934–938. CrossRef Medline

Huang YA, Maruyama Y, Stimac R, Roper SD (2008) Presynaptic (Type III) cells in mouse taste buds sense sour (acid) taste. J Physiol 586:2903–2912. CrossRef Medline

Huang YA, Dando R, Roper SD (2009) Autocrine and paracrine roles for ATP and serotonin in mouse taste buds. J Neurosci 29:13909–13918. CrossRef Medline

Huang YA, Pereira E, Roper SD (2011) Acid stimulation (sour taste) elicits GABA and serotonin release from mouse taste cells. PLoS One 6:e25471. CrossRef Medline

Huang YJ, Maruyama Y, Lu KS, Pereira E, Plonsky I, Baur JE, Wu D, Roper SD (2005) Mouse taste buds use serotonin as a neurotransmitter. J Neurosci 25:843–847. CrossRef Medline

Huang YJ, Maruyama Y, Dvoryanchikov G, Pereira E, Chaudhari N, Roper SD (2007) The role of pannexin 1 hemichannels in ATP release and cell-cell communication in mouse taste buds. Proc Natl Acad Sci U S A 104:6436–6441. CrossRef Medline

Ishida Y, Ugawa S, Ueda T, Yamada T, Shibata Y, Hondoh A, Inoue K, Yu Y, Shimada S (2009) P2X2- and P2X3-positive fibers in fungiform papillae originate from the chorda tympani but not the trigeminal nerve in rats and mice. J Comp Neurol 514:131–144. CrossRef Medline

Iwatsuki K, Ichikawa R, Hiasa M, Moriyama Y, Torii K, Uneyama H (2009) Identification of the vesicular nucleotide transporter (VNUT) in taste cells. Biochem Biophys Res Commun 388:1–5. CrossRef Medline

Jaber L, Zhao FL, Kolli T, Herness S (2014) A physiologic role for serotonergic transmission in adult rat taste buds. PLoS One 9:e112152. CrossRef Medline

Jackson MB, Yakel JL (1995) The 5-HT3 receptor channel. Annu Rev Physiol 57:447–468. CrossRef Medline

Jenkins A, Franks NP, Lieb WR (1996) Actions of general anaesthetics on 5-HT3 receptors in N1E-115 neuroblastoma cells. Br J Pharmacol 117: 1507–1515. CrossRef Medline

Kaya N, Shen T, Lu SG, Zhao FL, Herness S (2004) A paracrine signaling role for serotonin in rat taste buds: expression and localization of serotonin receptor subtypes. Am J Physiol Regul Integr Comp Physiol 286: R649–R658. CrossRef Medline

King MS, Bradley RM (2000) Biophysical properties and responses to glutamate receptor agonists of identified subpopulations of rat geniculate ganglion neurons. Brain Res 866:237–246. CrossRef Medline

Kinnamon JC, Taylor BJ, Delay RJ, Roper SD (1985) Ultrastructure of mouse vallate taste buds. I. Taste cells and their associated synapses. J Comp Neurol 235:48–60. CrossRef Medline

Mathes CM, Spector AC (2014) Systemic modulation of serotonergic synapses via reuptake blockade or 5HT1A receptor antagonism does not alter perithreshold taste sensitivity in rats. Chem Senses 39:583–593. CrossRef Medline

Meredith TL, Corcoran A, Roper SD (2015) Leptin's effect on taste bud calcium responses and transmitter secretion. Chem Senses 40:217–222. CrossRef Medline

Murata Y, Yasuo T, Yoshida R, Obata K, Yanagawa Y, Margolskee RF, Ninomiya Y (2010) Action potential-enhanced ATP release from taste cells through hemichannels. J Neurophysiol 104:896–901. CrossRef Medline

Nelson G, Chandrashekar J, Hoon MA, Feng L, Zhao G, Ryba NJ, Zuker CS (2002) An amino-acid taste receptor. Nature 416:199–202. CrossRef Medline

Nelson W, Halberg F (1973) An evaluation of time-dependent changes in susceptibility of mice to pentobarbital injection. Neuropharmacology 12: 509–524. CrossRef Medline

Ninomiya Y, Tonosaki K, Funakoshi M (1982) Gustatory neural response in the mouse. Brain Res 244:370–373. CrossRef Medline

Ninomiya Y, Higashi T, Katsukawa H, Mizukoshi T, Funakoshi M (1984a) Qualitative discrimination of gustatory stimuli in three different strains of mice. Brain Res 322:83–92. CrossRef Medline

Ninomiya Y, Mizukoshi T, Higashi T, Katsukawa H, Funakoshi M (1984b) Gustatory neural responses in three different strains of mice. Brain Res 302:305–314. CrossRef Medline

Ohkuri T, Horio N, Stratford JM, Finger TE, Ninomiya Y (2012) Residual chemoresponsiveness to acids in the superior laryngeal nerve in "taste-blind" (P2X2/P2X3 double-KO) mice. Chem Senses 37:523–532. CrossRef Medline

Oka Y, Butnaru M, von Buchholtz L, Ryba NJ, Zuker CS (2013) High salt recruits aversive taste pathways. Nature 494:472–475. CrossRef Medline

Romanov RA, Rogachevskaja OA, Bystrova MF, Jiang P, Margolskee RF, Kolesnikov SS (2007) Afferent neurotransmission mediated by hemichannels in mammalian taste cells. EMBO J 26:657–667. CrossRef Medline

Roper SD (2013) Taste buds as peripheral chemosensory processors. Semin Cell Dev Biol 24:71–79. CrossRef Medline

Rüsch D, Braun HA, Wulf H, Schuster A, Raines DE (2007) Inhibition of human 5-HT3A and 5-HT3AB receptors by etomidate, propofol and pentobarbital. Eur J Pharmacol 573:60–64. CrossRef Medline

Shin YK, Martin B, Golden E, Dotson CD, Maudsley S, Kim W, Jang HJ, Mattson MP, Drucker DJ, Egan JM, Munger SD (2008) Modulation of taste sensitivity by GLP-1 signaling. J Neurochem 106:455–463. CrossRef Medline

Takai S, Yasumatsu K, Inoue M, Iwata S, Yoshida R, Shigemura N, Yanagawa Y, Drucker DJ, Margolskee RF, Ninomiya Y (2015) Glucagon-like peptide-1 is specifically involved in sweet taste transmission. FASEB J 29:2268–2280. CrossRef Medline

Tomchik SM, Berg S, Kim JW, Chaudhari N, Roper SD (2007) Breadth of tuning and taste coding in mammalian taste buds. J Neurosci 27:10840–10848. CrossRef Medline

van Buskirk C (1945) The seventh nerve complex. J Comp Neurol 82:303–333. CrossRef

Vandenbeuch A, Anderson CB, Parnes J, Enjyoji K, Robson SC, Finger TE, Kinnamon SC (2013) Role of the ectonucleotidase NTPDase2 in taste bud function. Proc Natl Acad Sci U S A 110:14789–14794. CrossRef Medline

Vandenbeuch A, Larson ED, Anderson CB, Smith SA, Ford AP, Finger TE, Kinnamon SC (2015) Postsynaptic P2×3-containing receptors in gustatory nerve fibres mediate responses to all taste qualities in mice. J Physiol 593:1113–1125. Medline

Wang Z-Y, Keith IM, Olson EB Jr, Vidruk EH, Bisgard GE (2002) Expression of 5-HT3 receptors in primary sensory neurons of the petrosal ganglion of adult rats. Auton Neurosci 95:121–124. CrossRef Medline

Wu A, Dvoryanchikov G, Pereira E, Chaudhari N, Roper SD (2015) Breadth of tuning in taste afferent neurons varies with stimulus strength. Nat Commun 6:8171. CrossRef Medline

Yee CL, Yang R, Böttger B, Finger TE, Kinnamon JC (2001) "Type III" cells of rat taste buds: Immunohistochemical and ultrastructural studies of neuron-specific enolase, protein gene product 9.5, and serotonin. J Comp Neurol 440:97–108. CrossRef Medline

Zeitz KP, Guy N, Malmberg AB, Dirajlal S, Martin WJ, Sun L, Bonhaus DW, Stucky CL, Julius D, Basbaum AI (2002) The 5-HT3 subtype of serotonin receptor contributes to nociceptive processing via a novel subset of myelinated and unmyelinated nociceptors. J Neurosci 22:1010–1019. Medline